2008

Ligand induced ferromagnetism in ZnO nanostructures

Qian Wang
Southwest University, Virginia Commonwealth University

Qiang Sun
Peking University

P. Jena
Virginia Commonwealth University, pjena@vcu.edu

Wang, Q., Sun, Q., Jena, P. Ligand induced ferromagnetism in ZnO nanostructures. The Journal of Chemical Physics 129, 164714 (2008).

Ligand induced ferromagnetism in ZnO nanostructures

Qian Wang,[1,2] Qiang Sun,[3,a)] and P. Jena[2]
[1]*School of Physical Science and Technology, Southwest University, Chongqing 400715, China*
[2]*Department of Physics, Virginia Commonwealth University, Richmond, Virginia 23284, USA*
[3]*Department of Advanced Materials and Nanotechnology, Peking University, Beijing 100871, China and Center for Applied Physics and Technology, Peking University, Beijing 100871, China*

(Received 30 June 2008; accepted 19 September 2008; published online 30 October 2008)

Complementary to the experimental finding that ZnO nanoparticles become ferromagnetic when coated with N and S containing ligands such as dodecylamine and dodecanethiol [Garcia *et al.*, Nano Lett. **7**, 1489 (2007)], we provide the first theoretical understanding of the origin of magnetism in ligated ZnO nanoparticles as well as the structural properties of the ligated systems by using density functional theory and generalized gradient approximation for exchange and correlation, and a cluster model for the nanoparticles. We show that N or S atoms of the ligand bind to the Zn sites. The accompanying changes in the Zn–O bond length, hybridization between Zn $4s$ orbitals with N $2p$ or S $3p$ orbitals, and consequently the redistribution of charges between Zn and O atoms result in a magnetic system where the $2p$ electrons in O and N, and $3p$ electrons in S sites are spin polarized. Furthermore, the sites nearest to the Zn atom attached to the ligand carry bulk of the magnetic moment. Studies, as a function of cluster size, also illustrate that magnetism resides only on the surface. Our results confirm that the use of ligands can pave a new way for introducing magnetism in ZnO nanostructures, which can be used to develop magnetic sensors to detect N and S containing molecules. © *2008 American Institute of Physics*. [DOI: 10.1063/1.3001925]

I. INTRODUCTION

Recently there has been considerable interest in the study of dilute magnetic semiconductors as these systems offer the possibility of creating new electronics devices where the electron spin as well as its charge can be used. Among these systems, ZnO and GaN are the semiconductors of choice due to their large band gaps. In addition, ZnO[1–4] has many applications in spin functional devices, UV light emitters, varistors, transparent high power electronics, surface acoustic wave devices, piezoelectric transducers, gas-sensing, display, and solar cells. For magnetic functional devices, the ultimate goal of research is to make ZnO ferromagnetic at room temperature so that the spin as well as charge of the carriers can be coupled with an external magnetic field to produce new devices.

Until recently, the basic method for introducing magnetism into ZnO has been to dope it with transition metals such as V, Co, Cr, Mn, and Fe.[5–9] In these systems the magnetic moments are localized at the transition metal sites and carriers are needed to couple these moments. In spite of a great deal of work, both experimental and theoretical, transition metal doped ZnO materials have not lived up to their promise as dilute magnetic semiconductors for applications in spintronics. Much of the difficulties arise due to the strong dependence of experimental results on sample preparation conditions. It was recently found that ferromagnetism can also appear in undoped ZnO thin film[10] when Zn vacancies are introduced. The magnetization of very thin ZnO films was found to be much larger than that of the thicker films, suggesting that the vacancies must be located mostly at the surface. The origin of this magnetism has been shown theoretically[11] to be due to the unpaired $2p$ electrons at oxygen sites around the Zn vacancy. In addition, Zn vacancies prefer to occupy the surface sites, and the formation energy of Zn vacancy is higher than that of the oxygen vacancies.

The above studies suggest that a change in the electronic structure of ZnO alone can induce ferromagnetism and that it is not always necessary to dope ZnO with transition metal atoms. Further evidence to this hypothesis has come from recent experiments where ZnO nanoparticles coated with different organic molecules[12] such as dodecylamine, dodecanethiol, and tryoctylphosphine have been found to be ferromagnetic. However, a fundamental understanding of the origin of ligand induced ferromagnetism is lacking. For example, how are the electronic structure and geometry of ZnO nanoparticles modified upon ligand capping? What is the origin of ferromagnetism and which sites carry the magnetic moment? Does magnetism reside only on the surface of the particle or does it permeate throughout its interior? How do the ligands bind to the ZnO nanoparticle? In this paper, we have carried out a first principles theoretical study to address these questions.

II. COMPUTATIONAL PROCEDURE

The calculations were performed using the generalized gradient approximation (GGA) to the density functional theory. The GGA functional by Perdew–Wang[13] and double numeric basis sets, supplemented with polarization functions, were used. Spin-polarized self-consistent field calculations with a convergence criterion of 10^{-6} a.u. for total energies were carried out using the DMOL3 package.[14]

a)Electronic mail: sunq@coe.pku.edu.cn.

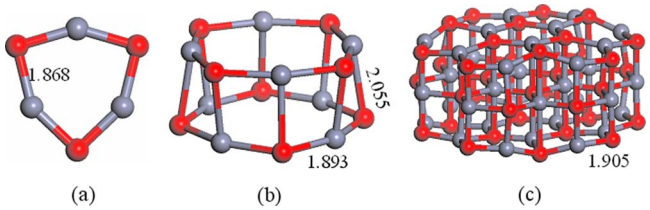

FIG. 1. (Color online) Optimized geometry of (a) Zn_3O_3, (b) Zn_8O_8, and (c) $Zn_{36}O_{36}$.

Geometry optimization was performed using the Broyden–Fletcher–Goldfarb–Shanno algorithm with a convergence criterion of 1×10^{-3} a.u. for the maximum force and 4×10^{-3} Å for the maximum displacement.

We note that experiments are carried out on ZnO nanoparticles having a size of about 10 nm. The ligands such as dodecylamine ($C_{12}H_{27}N$) and dodecanethiol ($C_{12}H_{25}SH$) that are used to cap these nanoparticles also have large molecular weights, namely, 185.3 and 202.4, respectively. Since it is computationally impossible to fully optimize ligated particles of these sizes using first principles techniques, we have used a cluster model where Zn_xO_x (x=3, 8, 36) clusters represent ZnO nanoparticles and NH_2 and SCH_3 functional groups represent dodecylamine ($C_{12}H_{27}N$) and dodecanethiol ($C_{12}H_{25}SH$) ligands, respectively. We should point out that very small clusters of metal oxides and metal halides have been shown to possess the essential physics and chemistry of their respective bulk due to the strong covalent bonding.[15] In addition, by studying the magnetic properties of ZnO clusters as a function of size, we are able to determine how their properties depend on size and topology and whether magnetism is associated with atoms only on the surface or those in the bulk.

III. RESULTS AND DISCUSSIONS

A. Geometries of Zn_xO_x (x=3, 8, 36) clusters

We begin with the optimized structures of Zn_xO_x (x=3, 8, 36) clusters. The ground state structure of Zn_3O_3 has been found[16,17] to be ringlike with D_{3h} symmetry as shown in Fig. 1(a), where the Zn–O bond length is 1.868 Å. Note that the Zn–O distance in bulk ZnO is 1.978 Å. Zn_8O_8, on the other hand, has been found to be a tubelike structure composed of two eight-membered rings, as given in Fig. 1(b). Here the Zn–O bond lengths vary between 1.893 and 2.055 Å. In both structures all the Zn and O atoms are surface atoms and the Zn atoms do not possess the tetrahedral bonding characteristic of bulk ZnO nor of a particle of the size of 10 nm. To simulate a more realistic nanoparticle, we have used a $Zn_{36}O_{36}$ cluster by cutting a small piece from bulk ZnO with wurtzite structure. The cluster was then fully optimized with out any symmetry constraints. The resulting optimized geometry of $Zn_{36}O_{36}$ cluster is shown in Fig. 1(c). We see that the structural skeleton of the cluster is still kept except for bond length contraction of surface atoms due to finite size effect. The average Zn–O bond length on the surface is 1.935 Å, which is contracted by 12% as compared to that of inside ones. All the above Zn_xO_x clusters are found to be in a spin singlet state, i.e., nonmagnetic as expected.

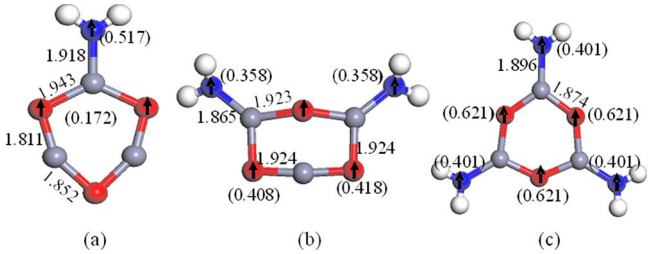

FIG. 2. (Color online) Optimized geometry of (a) $Zn_3O_3(NH_2)_1$, (b) $Zn_3O_3(NH_2)_2$, and (c) $Zn_3O_3(NH_2)_3$. The numbers with and without parentheses represent magnetic moments and bond lengths, respectively.

B. Zn_xO_x (x=3, 36) clusters ligated with NH_2 functional group

We first consider the interaction of NH_2 with Zn_3O_3. There are a number of sites where NH_2 can be attached to Zn_3O_3. The possible configurations are top of a Zn atom, top of an O atom, bridge site on a Zn–O bond, or the hollow site of the ring. We found that the most stable site for the NH_2 group is the on-top Zn site, as shown in Fig. 2(a), which is 0.64 eV lower in energy than that of Zn–O bridge site. The binding energy of NH_2 with Zn_3O_3 is found to be 1.463 eV. The Zn–O bond nearest to the N site is elongated to 1.918 Å, while the next nearest bond shrinks slightly to 1.811 Å. The farthest Zn–O bond essentially remains unaltered. This suggests that the effect of the ligand is localized.

The expansion of the Zn–O bond nearest to the N atom is due to the charge redistribution caused by the ligand. As the Zn atom transfers part of its charge to the N atom, the charge transfer to the neighboring O atoms decreases, thus weakening the Zn–O bond while simultaneously creating a hole in the O $2p$ orbital. This charge redistribution gives rise to the magnetic properties of the $Zn_3O_3NH_2$ cluster. While Zn_3O_3 is nonmagnetic, i.e., a spin singlet, introduction of NH_2 group leads to a ferromagnetic cluster where N site carries a moment of $0.517\mu_B$ and the two O sites closest to the NH_2 group carry a moment of $0.172\mu_B$ each. The moments on other two O sites ($0.046\mu_B$), Zn sites ($0.005\mu_B$), and H sites ($0.012\mu_B$) are negligible. The total magnetic moment of $Zn_3O_3NH_2$ is $1\mu_B$. To examine if the two O atoms closest to the NH_2 group would rather couple antiferromagnetically, we calculated the total energy of the $Zn_3O_3NH_2$ cluster by allowing the main sites (O–N–O) to have the ($\uparrow\uparrow\downarrow$) spin alignment. We found this configuration to be 35 meV higher in energy than the ($\uparrow\uparrow\uparrow$) configuration. This suggests that the system prefers to be ferromagnetically coupled.

We should point out that $Zn_3O_3NH_2$ is an odd electron system and at the very minimum it will have a magnetic moment of $1\mu_B$, which is what we have found. Even though the preferred spin configuration of this cluster shows that the two O atoms nearest to the ligand are spin polarized in the parallel direction, one cannot firmly conclude that this cluster is ferromagnetic. We have, therefore, studied the magnetic properties of $Zn_3O_3(NH_2)_2$ and $Zn_3O_3(NH_2)_3$ clusters. The former is an even-electron system and thus has the potential to be a spin singlet, and hence nonmagnetic while the later could have a total moment of $1\mu_B$ or $3\mu_B$. We find that the

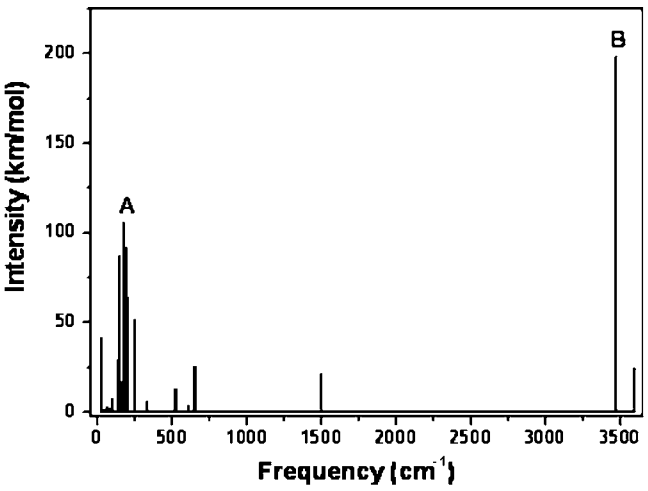

FIG. 3. Vibrational spectra of $Zn_3O_3(NH_2)_3$.

total magnetic moments of $Zn_3O_3(NH_2)_2$ and $Zn_3O_3(NH_2)_3$ clusters are $2\mu_B$ and $3\mu_B$, respectively. Thus, one can conclude that NH_2 ligands have transformed nonmagnetic Zn_3O_3 clusters into ferromagnetic ones.

We provide some details of the structure and spin alignment of $Zn_3O_3(NH_2)_2$ and $Zn_3O_3(NH_2)_3$ clusters in the following. In Figs. 2(b) and 2(c) we plot the fully optimized geometries of the above clusters. We see from Figs. 2(b) and 2(c) that the Zn–O bonds nearest to the N atom are 1.923 and 1.874 Å for $Zn_3O_3(NH_2)_2$ and $Zn_3O_3(NH_2)_3$, respectively. The latter one is very close to 1.868 Å distance in the Zn_3O_3 cluster. The Zn–N bond lengths are,respectively,1.865 and 1.874 Å, which are smaller than that in the $Zn_3O_3NH_2$ cluster. The binding energies per NH_2 group in Figs. 2(b) and 2(c) were found to be 1.455 and 1.444 eV, respectively, which are almost unchanged from the binding energy of 1.463 eV when the first NH_2 group was attached. The systems remain magnetic with a total moment of $2\mu_B$ and $3\mu_B$, although the distribution of magnetic moments is changed. Each N site carries $0.358\mu_B$ and $0.40\mu_B$, and each O site carries $0.408\mu_B$ and $0.621\mu_B$ in $Zn_3O_3(NH_2)_2$ and $Zn_3O_3(NH_2)_3$, respectively.

To verify the magnetic stability of the system, we have calculated the spin gaps: $\delta_1 = -(E^+_{\mathrm{HOMO}} - E^-_{\mathrm{LUMO}})$ and $\delta_2 = -(E^-_{\mathrm{HOMO}} - E^+_{\mathrm{LUMO}})$, where (+) represents spin-up and (−) represents spin-down levels. We find δ_1 and δ_2 to be 0.12 and 0.15 eV in $Zn_3O_3(NH_2)_3$, respectively. The spin gap corresponds to the energy required to move an infinitesimal amount of charge from the highest occupied molecular orbital (HOMO) of one spin to the lowest unoccupied molecular orbital (LUMO) of the other. Positive values for both spin gaps guarantee that the system is stable magnetically as well as electronically. To further check the dynamic stability of the geometry, we calculated the vibrational spectra, as shown in Fig. 3. Peak A is mainly contributed by O and Zn atoms, while peak B is by H atoms. There is no imaginary frequency in any of the 39 vibrational modes, so the geometry itself is dynamically stable.

The analysis of electronic structure indicates that for Zn_3O_3 the HOMO is mainly contributed by O atoms and LUMO by Zn atoms. However, after capping this cluster with NH_2 groups the HOMO and LUMO are predominately contributed by N atoms in the NH_2 groups. Moreover, charge analysis suggests that ligand capping reduces the charge transfer from Zn to O. As discussed earlier, this not only affects the covalent bonding features between Zn and O but also produces some holes in O $2p$ orbitals, thus causing magnetism to appear.

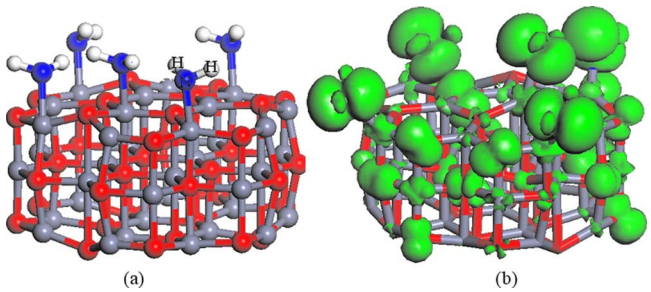

FIG. 4. (Color online) (a) Geometry and (b) spin density of $Zn_{36}O_{36}(NH_2)_5$.

As pointed out earlier, the above cluster does not fully represent the size of nanoparticles studied experimentally as the Zn atoms in Zn_3O_3 cluster do not have the tetrahedral bonding expected in large nanoparticles. We have, therefore, repeated the above calculations using a larger cluster of $Zn_{36}O_{36}$, as shown in Fig. 1(c). Due to the limited space, it is difficult to cap the functional group on each Zn site in the surface. As an example, here we study the case of capping five NH_2 functional groups. The optimized geometry is given in Fig. 4(a). We find the average binding energy per NH_2 to be 1.40 eV, which is a little bit smaller than that in Zn_3O_3. The average N–Zn bond length is 2.03 Å, and the Zn–O bond length involved is slightly elongated. It is important to note that the total magnetic moment of this system is $5\mu_B$, mainly contributed from $2p$ orbitals of N and O surface atoms, as shown by spin density in Fig. 4(b). The magnetic behavior of this capped ZnO is further confirmed by the spin density of states (DOS) in Fig. 5, where the dotted line indicates the Fermi energy. For comparison we also plot the total DOS and partial DOS of Zn and O atoms at the surface site and bulklike site, respectively, for pure $Zn_{36}O_{36}$. The total DOS shows that the DOSs for spin-up and spin-down states are symmetric, and hence the system is nonmagnetic. From the partial DOSs, we clearly see that the surface states above the valence band maximum for both Zn and O atoms at the surface sites and Zn atom does not contribute much to the DOS near the Fermi energy. After five NH_2 groups are capped on the surface, the spin-up states are shifted up, resulting in a magnetic system. The partial DOSs for p orbitals of the surface O and N atoms are also given in Fig. 5, where the exchange splitting can be clearly seen.

C. Zn_xO_x (x=3, 8) clusters ligated with SCH_3 functional group

Next we study the effects of SCH_3 ligands. Following the same procedure as for NH_2, we find that the stable site for ligand binding is again the on-top Zn site, as shown in Fig. 6(a). The bond length of Zn–S is 2.263 Å and is larger than the Zn–N bond in Zn_3O_3-$3NH_2$. The binding energy per

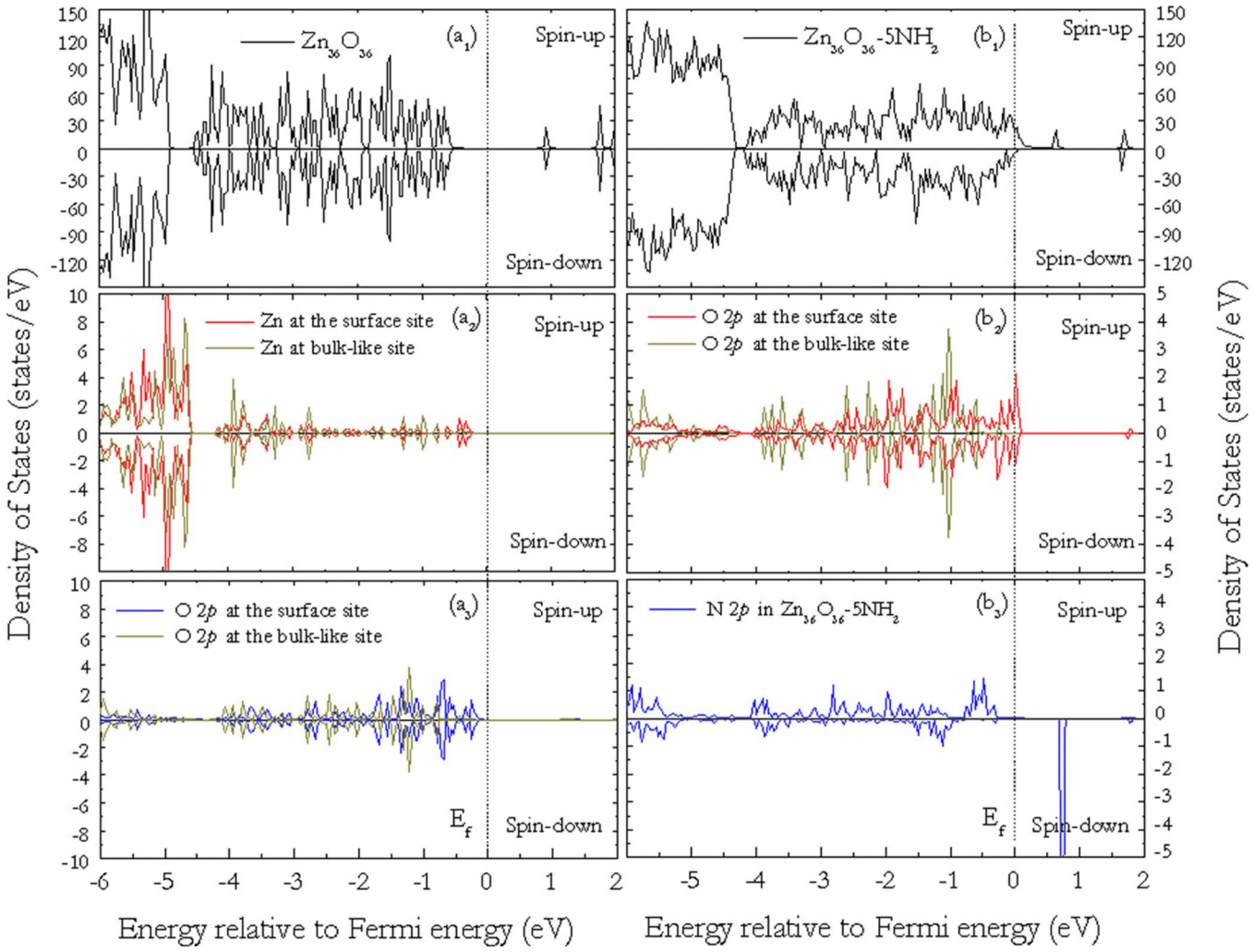

FIG. 5. (Color online) $[(a_1)-(a_3)]$ Total spin DOS, partial DOS of Zn at the surface site and bulklike site, and partial DOS of O $2p$ at the surface site and bulklike site in $Zn_{36}O_{36}$. $[(b_1)-(b_3)]$ Total DOS, partial DOS of O $2p$ at the surface site and bulklike site, and partial DOS of N $2p$ in $Zn_{36}O_{36}(NH_2)_5$.

SCH_3 unit is 1.354 eV, which is a little bit smaller than that of NH_2 unit (1.444 eV). The possible reason is that N has a larger electronegativity than S does and Zn–N bond length is shorter than Zn–S bond. On the other hand, the Zn–O bond length of 1.872 Å is almost unchanged from that in Zn_3O_3-3NH_2. Some differences exist in magnetism and electronic structure. In this case, each S site carries a moment of $0.371\mu_B$, and each O site carries a moment of $0.571\mu_B$, smaller than the moments in Zn_3O_3-3NH_2. The total magnetic moment of Zn_3O_3-3SCH_3 is $3\mu_B$. The HOMO is mainly from $3p$ orbitals of S atoms, and LUMO from $2p$ orbitals of O atoms, as shown in Figs. 6(b) and 6(c).

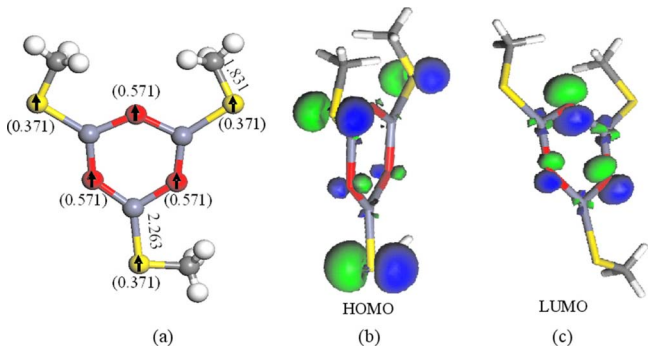

FIG. 6. (Color online) (a) Geometry, (b) HOMO, and (c) LUMO of $Zn_3O_3(SCH_3)_3$.

To study the effect of cluster geometry on magnetism when capped with S containing ligand, we have chosen Zn_8O_8, which has been found to be a tubelike structure composed of two eight-membered rings, as given in Fig. 1(b). When eight SCH_3 units are capped on Zn_8O_8, the structure changes very little from that in Fig. 1(b). The optimized structure of $Zn_8O_8(SCH_3)_8$ is shown in Fig. 7(a). Once again, $Zn_8O_8(SCH_3)_8$ is magnetic where each S site has a moment of $0.559\mu_B$, and each O site has a moment of $0.416\mu_B$. The total magnetic moment of $Zn_8O_8(SCH_3)_8$ is $8\mu_B$. The individual magnetic moments at S and O sites are larger than those in Zn_3O_3-3SCH_3. One of the possible reasons for this enhancement is that due to the tubular shape of Zn_8O_8, SCH_3 capping expands the Zn–O bond length, which in turn leads to enhancement in the magnetic moments. The spin density plot given in Fig. 7(b) clearly shows the p-orbital characteristics. This is totally different from the origin of magnetism in transition metal doped ZnO, where the localized $3d$ orbitals of dopants contribute to the observed magnetism.

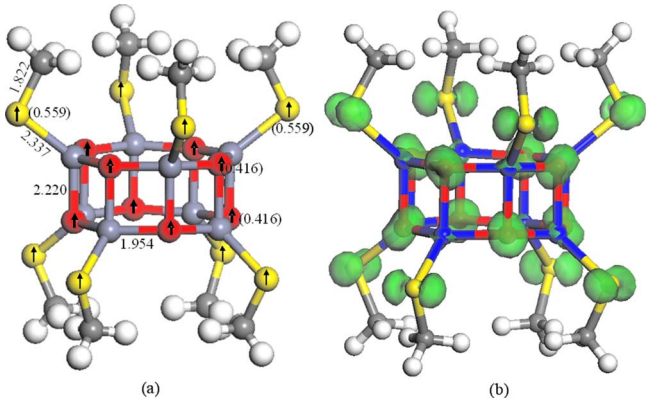

FIG. 7. (Color online) (a) Geometry and (b) induced spin density in $Zn_8O_8(SCH_3)_8$.

IV. SUMMARY OF CONCLUSIONS

In summary, we have provided a theoretical understanding of the origin of magnetism in ligated ZnO nanostructures. Based on the results of Zn_3O_3 with ring structure, Zn_8O_8 with tubelike structure, and $Zn_{36}O_{36}$ with bulklike structure, we find that the induced magnetism is an intrinsic property of ligated ZnO nanostructures containing N or S groups. Ligand capping causes redistribution of charges in Zn, O, and N or S sites. The resulting unpaired *p* electrons in O, N, and S sites lead to the magnetic moments and make the system magnetic. Our results are in agreement with recently observed magnetism in ligated ZnO.[12] There are some important potential applications of ligand induced magnetic materials in magnetic sensor and biomedicine. For example, (1) the magnetic signal can be used for sensing some S-containing or N-containing molecules, which are easily formed in automotive engines, in industrial combustion systems, or in chemical feedstocks. Because most of these molecules are very harmful and poisonous, developing new sensors with high sensitivity for these molecules are desirable; (2) the ligand induced magnetism in combination with biocompatibility of ZnO itself offers some possibilities that ligated ZnO nanoparticles may have applications in magnetic healing, targeted delivery, and effective biofluid circulations.

ACKNOWLEDGMENTS

This work was supported in part by grants from the National Natural Science Foundation of China (No. 10744006) and from the (U.S.) Department of Energy.

[1] L. S. Mende and J. L. MacManus-Driscoll, Mater. Today **10**, 40 (2007).
[2] X.-D. Wang, J.-H. Song, and Z. L. Wang, Science **316**, 102 (2007).
[3] J. Zhou, N. Xu, and Z. L. Wang, Adv. Mater. (Weinheim, Ger.) **18**, 2432 (2006).
[4] A. Tsukazaki, A. Ohtomo, T. Kita, Y. Ohno, H. Ohno, and M. Kawasaki, Science **315**, 1388 (2007).
[5] Q. Wang, Q. Sun, P. Jena, Z. Hu, R. Note, and Y. Kawazoe, Appl. Phys. Lett. **91**, 063116 (2007).
[6] K. R. Kittilstved, D. A. Schwartz, A. C. Tuan, C. M. Heald, S. A. Chambers, and D. R. Gamelin, Phys. Rev. Lett. **97**, 037203 (2006).
[7] M. Venkatesan, C. B. Fitzgerald, J. G. Lunney, and J. M. Coey, Phys. Rev. Lett. **93**, 177206 (2004).
[8] P. Sati, C. Deparis, C. Morhain, S. Schäfer, and A. Stepanov, Phys. Rev. Lett. **98**, 137204 (2007).
[9] Q. Wang, Q. Sun, P. Jena, and Y. Kawazoe, Appl. Phys. Lett. **87**, 162509 (2005).
[10] N. H. Hong, J. Sakai, and V. Brize, J. Phys.: Condens. Matter **19**, 036219 (2007).
[11] Q. Wang, Q. Sun, G. Chen, Y. Kawazoe, and P. Jena, Phys. Rev. B **77**, 205411 (2008).
[12] M. A. Garcia, J. M. Merino, E. F. Pinel, A. Quesada, J. de la Venta, M. L. Ruíz González, G. R. Castro, P. Crespo, J. Llopis, J. M. González-Calbet, and A. Hernando, Nano Lett. **7**, 1489 (2007).
[13] J. P. Perdew, K. Burke, and M. Ernzerhof, Phys. Rev. Lett. **77**, 3865 (1996).
[14] B. Delley, J. Chem. Phys. **92**, 508 (1990).
[15] A. W. Castleman and P. Jena, Proc. Natl. Acad. Sci. U.S.A. **103**, 10554 (2006).
[16] J. M. Matxain, J. M. Mercero, J. E. Fowler, and J. M. Ugalde, J. Am. Chem. Soc. **125**, 9494 (2003).
[17] J. M. Matxain, J. E. Fowler, and J. M. Ugalde, Phys. Rev. A **62**, 053201 (2000).